Article

*J. Biol. Regul. Homeost. Agents.* 2024; 38(5): 4415–4426
https://doi.org/10.23812/j.biol.regul.homeost.agents.20243805.351

# Salidroside Improves Cellular Senescence in COPD by Inhibiting the JAK2/STAT3 Pathway

Leping Li[1], Wenli Fu[1], Juan Wang[1], Sha Zhang[1], Weiying Liu[2,*]

[1]Department of Respiratory Medicine, The First Clinical Medical College of Lanzhou University, 730000 Lanzhou, Gansu, China
[2]Department of Respiratory and Critical Care Medicine, The First Hospital of Lanzhou University, 730000 Lanzhou, Gansu, China
*Correspondence: lwy70828@126.com (Weiying Liu)
Published: 1 May 2024

**Background: Chronic obstructive pulmonary disease (COPD) is a respiratory illness, with cellular senescence recognized as an essential mechanism driving this chronic lung disease. Salidroside (Sal), a natural compound, is recognized for its anti-aging impacts. Therefore, this study aims to investigate the role and the underlying mechanism of Sal on airway epithelial cell senescence.**

**Methods: *In vitro* experiments were performed by treating BEAS-2B cells with cigarette smoke extract (CSE), AG490 (Janus kinase 2 (JAK2) inhibitor), or Sal (40 µM, 80 µM, 160 µM). Moreover, senescence-associated $\beta$-galactosidase (SA-$\beta$-gal) staining and the manifestation of senescence-related genes were used to assess cellular senescence. The mRNA levels of cyclin-dependent kinase inhibitor 2a (*p16*) and cyclin-dependent kinase inhibitor 1a (*p21*) were evaluated. Furthermore, Western blot analysis was employed to determine the expression levels of p16, p21, Janus kinase 2 (JAK2), phosphorylated-JAK2 (p-JAK2), signal transducer and activator of transcription 3 (STAT3), and phosphorylated-STAT3 (p-STAT3). Additionally, the cytokine levels associated with the senescence-associated secretory phenotype (SASP) were evaluated utilizing corresponding enzyme-linked immunosorbent assay kits.**

**Results: *In vitro*, cellular experiments demonstrated that Human bronchial epithelial cells underwent senescence in response to CSE, as evidenced by elevated expression of p16 ($p < 0.05$) and p21 ($p < 0.05$), and promotion of senescence-associated secretory phenotype (SASP), as well as up-regulation of JAK2/STAT3 signaling pathway activity. AG490 treatment significantly ameliorated CSE-induced cellular senescence, resulting in down-regulation of the JKA2/STAT3 signaling pathway, alleviation of the senescence molecules p16 ($p < 0.05$), p21 ($p < 0.05$), p-JKA2 ($p < 0.01$) and p-STAT3 ($p < 0.05$). The inhibitor decreased the secretion of SASP cytokines, and decreased the activity of SA-$\beta$-gal. Additionally, Sal reduced p16 ($p < 0.01$) and p21 ($p < 0.05$) expression, potentially reversed CSE-induced cellular senescence, and inhibited the JAK2/STAT3 signaling pathway, as well as decreased SASP secretion and SA-$\beta$-gal activity.**

**Conclusion: Sal reduces CSE-induced BEAS-2B cellular senescence by inhibiting the JAK2/STAT3 signaling pathway, providing a novel strategy for COPD treatment.**

**Keywords:** salidroside; JAK2; STAT3; cellular senescence

## Introduction

Chronic obstructive pulmonary disease (COPD), a respiratory illness with a significant rate of morbidity and mortality, imposes a substantial disease burden on individuals [1]. It is characterized by persistent low-grade lung inflammation, progressive airflow constriction, and irreversible damage to lung parenchymal tissue [2]. Cigarette smoke (CS) exposure is a significant risk factor for COPD. A large body of evidence indicates a strong association between COPD and lung aging, with cellular senescence recognized as an essential mechanism driving this chronic lung disease [3,4]. CS can mediate the release of excess oxidants and reactive oxygen species (ROS) [5], promoting the activation of the tumor protein p53/cyclin-dependent kinase inhibitor 1a (p53/p21) or cyclin-dependent kinase inhibitor 2a/retinoblastoma (p16/RB) pathways, which induce cell cycle arrest and aging [6]. However, senescent cells remain metabolically active and continue to secrete a specific set of molecules known as the senescence-associated secretory phenotype (SASP), which includes interleukin-6 (IL-6), interleukin-8 (IL-8) and matrix metalloproteinase (MMP) [7]. SASP is a hallmark of cellular senescence, leading to chronic, low-grade inflammation in COPD. This inflammation exacerbates the deterioration of lung function and ultimately accelerates lung aging [8]. Therefore, drugs with anti-aging effects hold great potential to prevent the development of COPD.

Janus kinase 2/signal transducer and activator of transcription 3 (JAK2/STAT3), an essential signaling pathway in the JAK/STAT pathway, plays a pivotal role in cell growth, differentiation, proliferation, and apoptosis and is

Journal of
BIOLOGICAL REGULATORS
and Homeostatic Agents

implicated in the expansion of many diseases [9]. Within the cytoplasm, activated phosphorylated tyrosine kinase 2 (p-JAK2) phosphorylates Tyr1007 and Tyr1008 formed STAT3 docking sites, leading to the aggregation of STAT3 binding sites [10]. STAT3 translocates as a dimer from the cytoplasm to the nucleus, which is essential for the transcription of the proinflammatory cytokine and influences the expression of associated downstream chemokines [11]. JAK plays an essential role in the production of SASP [12–14]. Wu *et al*. [15] demonstrated that estrogen-mediated SASP factors promote the senescence of mesenchymal stem cells (MSCs) through the JAK2/STAT3 signaling pathway. Zhou *et al*. [16] found that blocking the JAK2/STAT pathway could delay the senescence of human glomerular thylakoid cells. Inhibition of the JAK2/STAT3 signaling pathway decreases the secretion of the SASP factor in osteoblasts, thereby alleviating osteoporosis [17]. In Alzheimer disease's transgenic mice models, baicalin suppresses the activation of the JAK2/STAT3 signaling pathway triggered by A$\beta$-induced microglia control [18]. Furthermore, p53/p21 is a direct target of STAT3, and the reduced level of SASP factor prevents the proliferation of senescent cells [19]. Therefore, the JAK2/STAT3 signaling pathway is closely linked to senescence. However, it remains unclear whether JAK2/STAT3 participates in cigarette smoke extract (CSE)-induced senescence in bronchial epithelial cells.

Salidroside (Sal) is one of the main components of rhodiola rosea extract, known for its diverse pharmacological effects, including anti-aging, anti-inflammatory, antioxidant, and anticancer properties [20]. Sal reduces age-related cognitive decline in Alzheimer disease (AD) rats through modulation of the phosphoinositide 3 kinase/protein kinase b (PI3K/AKT) signaling pathway [21]. Additionally, Sal has been shown to improve neuronal damage in Parkinson's Disease mice by inhibiting nod-like receptor thermal protein domain-associated protein 3 (NLRP3)-dependent cellular death [22]. Sun *et al*. [23] reported that Sal treatment reduced the upregulation of senescence-related genes *p53* and *p21* in ox-LDL-treated EA. hy926 cells, thereby hindering the progression of endothelial cell senescence. Previous report has shown that Sal inhibits the expression of p16 and p21 induced by $H_2O_2$ in human umbilical vein endothelial cells (HUVECs) and reduces senescence-associated $\beta$-galactosidase (SA-$\beta$-gal) activity [24]. Furthermore, Sal attenuated ultraviolet radiation B-induced senescence in human dermal fibroblasts (HDFS) by decreasing SA-$\beta$-gal activity and hindering cell cycle arrest [25]. However, whether Sal alleviates senescence triggered by CSE in BEAS-2B cells remains unknown. Therefore, this study aims to investigate whether Sal regulates CSE-induced cellular senescence through modulation of the JAK2/STAT3 signaling pathway.

## Materials and Methods

### *Preparation for CSE*

CSE's approach was performed as previously described [26], involved using a vacuum pump (GL-802A, Kylin-Bell, Haimen, China) to gulp smoke from an unfiltered cigarette (Red Lanzhou, Gansu Tobacco, Lanzhou, China). The smoke was drawn into 30 mL of Dulbecco's Modified Eagle Medium (DMEM) (BL301A, Biosharp, Hefei, China) for 1 minute and subsequently underwent sterilization by passing CSE solution through a 0.22 µm filter (SLGP033RB, Millipore, Burlington, MA, USA). After filtration, sodium hydroxide was employed to adjust the pH to 7.4 within 30 minutes of preparation, establishing a 100% CSE solution. This solution was diluted to the desired concentration with a medium for each experiment.

### *Cell Culture*

BEAS-2B cell line (CL-0496, Procel, Wuhan, China) is a human epithelial cell transformed with an adenovirus 12-SV 40 virus hybrid, isolated from a normal human bronchial epithelial cell line obtained during necropsy of non-cancerous individuals. Cells used in this study were authenticated using STR profiling, and there was no cross-contamination between cells following mycoplasma testing. The cells were maintained in DMEM medium supplemented with 10% FBS and 1% penicillin/streptomycin followed by incubation at 37 °C in 5% $CO_2$. Sal was purchased from Shanghai Yuanye Biotechnology Co. Ltd (10338-51-9, Shanghai, China), and BEAS-2B cells were exposed to varying concentrations (40 µM, 80 µM, and 160 µM) of Sal for 8 hours or 10 µM of AG490 (S1143, Selleck, Houston, TX, USA) for 2 hours, before the addition of different concentrations of CSE.

### *Cell Counting Kit-8 (CCK-8) Assay*

BEAS-2B cells were inoculated in 96-well plates at a density of $1 \times 10^4$ cells/well and subsequently exposed to different concentrations of CSE (0, 1%, 3%, 5%, 7%, 9%, and 11%) for 24 hours. After 24 hours of incubation, 10 µL of CCK-8 (AR1160, BOSTOR, Wuhan, China) was added and incubated for 2 hours in the dark. The absorbance value of each group of cells was assessed at 450nm using an enzyme labeling instrument (Multiskan FC, Thermo Fisher, Waltham, MA, USA). For statistical significance, each experiment was independently repeated three times. Furthermore, the impact of different concentrations of Sal (0, 5 µM, 10 µM, 20 µM, 40 µM, 80 µM, 160 µM, 320 µM) on the viability of BEAS-2B cells was determined as follows: Cell viability = $(OD_{treatment} - OD_{blank})/OD_{control} - OD_{blank})$ 100%.

### *SA-$\beta$-gal Staining*

The SA-$\beta$-gal activity was ascertained using the SA-$\beta$-gal staining kit (C0602, Beyotime, Shanghai, China).

**Table 1. A list of primers used in qRT-PCR.**

| Genes | Sequences (5′-3′) |
|---|---|
| *p16*-human | Forward: CTCTGAGAAACCTCGGGAAACT |
| *p16*-human | Reverse: AACTACGAAAGCGGGGGTGG |
| *p21*-human | Forward: TGTCTTGTACCCTTGTGCCT |
| *p21*-human | Reverse: TGGTAGAAATCTGTCATGCTGGTC |
| *GAPDH*-human | Forward: CAGGAGGCATTGCTGATGAT |
| *GAPDH*-human | Reverse: GAAGGCTGGGGGCTCATTT |

qRT-PCR, quantitative real-time polymerase chain reaction; *p16*, cyclin dependent kinase inhibitor 2a; *p21*, cyclin dependent kinase inhibitor 1a; *GAPDH*, glyceraldehyde-3-phosphate dehydrogenase.

Initially, BEAS-2B cells were seeded into a 6-well plate at a density of $2 \times 10^5$ cells/well and subsequently treated with CSE, Sal, or AG490. The cells were then fixed for 15 minutes at room temperature, followed by three times PBS washes, and underwent treatment with 1 mL of $\beta$-galactosidase staining solution. After overnight incubation at 37 °C without $CO_2$, the cells were observed using an ordinary light microscope (IX73, Olympus, Tokyo, Japan). The percentage of SA-$\beta$-gal positive cells was obtained using imageJ software (version 1.8.0, NIH, Bethesda, MD, USA) and experiments were averaged in triplicate.

### *Quantitative Real-Time Polymerase Chain Reaction (qRT-PCR) Assay*

Total RNA from the cell samples was extracted employing a Trizol kit (9108, Takara, Osaka, Japan). Subsequently, RNA was converted into cDNA using the PrimeScriptTM RT kit (RR047A, Takara, Osaka, Japan). qRT-PCR was performed utilizing the SYBR premixed Ex TaqTM II kit (RR820A, Takara, Osaka, Japan) on the ABI system (QuantStudio 3, ABI, Waltham, MA, USA). The relative expression of target genes was conducted employing the $2^{-\Delta\Delta Ct}$ method. The list of primers obtained from Singke, Beijing, China, is shown in Table 1.

### *Western Blot Analysis*

Total cellular protein was extracted using radioimmunoprecipitation Assay (RIPA) lysis buffer (R0010, Solarbio, Beijing, China). The proteins were resolved through sodium dodecyl sulfate-polyacrylamide gel electrophoresis (SDS-PAGE) and subsequently transferred onto a polyvinylidene fluoride (PVDF) membrane. The membranes were blocked with 5% skim milk for 1 hour. The membrane was incubated overnight at 4 °C with primary antibodies against p16 (10883-1-AP, 1:1000, Proteintech, Wuhan, China), p21 (#2947, 1:1000, CST, Denver, MA, USA) and JAK2 (ab108596, 1:1000, Abcam, Cambridge, UK), phosphorylated-JAK2 (p-JAK2) (ab32101, 1:1000, Abcam, Cambridge, UK), STAT3 (ab68153, 1:2000, Abcam, Cambridge, UK), and phosphorylated-STAT3 (p-STAT3) (ab76315, 1:2000, Abcam, Cambridge, UK). The next day, the membrane was washed using tris buffered saline and tween 20 (TBST) buffer and incubated with HRP labeled secondary antibody and goat anti-rabbit IgG (LF102, 1:8000, EpiZyme, Shanghai, China) at ambient temperature for one hour. Finally, the immunoblots were developed using a chemiluminescence kit (SQ201, EpiZyme, Shanghai, China) and quantitatively analyzed through ImageJ software. Moreover, glyceraldehyde-3-phosphate dehydrogenase (GAPDH) (LF206, 1:10,000, EpiZyme, Shanghai, China) served as an internal control.

### *Cytokine Measurements*

The enzyme-linked immunosorbent assay (ELISA) was utilized to determine the levels of IL-1$\beta$ (HJ064, EpiZyme, Shanghai, China), IL-8 (HP-Elisa, Hepenbio, Suzhou, China), and MMP2 (ml058669-2, Mibio, Beijing, China) in the supernatant of cell cultures, following the guidelines provided with the corresponding ELISA kits. The absorbance was assessed at 450 nm and compared with the enzyme marker.

### *Bioinformatics Analysis*

COPD gene expression data were collected from the GEO database (https://www.ncbi.nlm.nih.gov/geo/). The GPL4133 platform-based GSE38974 dataset included mRNA expression data from 23 COPD samples and 9 control samples. The dataset was used to explore the differential expression levels of certain genes. Furthermore, a nomogram of the differentially expressed genes was constructed using the "Rms" R [27], where the "Points" correspond to the scores assigned to the candidate genes, while the "Total Points" represent the sum of each person's points for all these genes. Additionally, the diagnostic significance was evaluated by computing the area under the curve (AUC) and 95% confidence interval (CI) using receiver operating characteristic (ROC) curves and line plots. AUC $>0.7$ indicates an effective diagnostic criterion.

### *Statistical Analysis*

GraphPad Prism (version 9.5.0, GraphPad Software, San Diego, CA, USA) was used for statistical analysis. For statistical significance, each experiment was independently repeated three times, and the data were expressed as the mean $\pm$ standard deviation (SD). The comparison between the two groups was performed using the independent sample *t*-test. Moreover, the multi-group comparison was conducted through a one-way analysis of variance (ANOVA) followed by Tukey's test. Statistical significance was achieved at a $p$-value $< 0.05$.

Journal of
BIOLOGICAL REGULATORS
and Homeostatic Agents

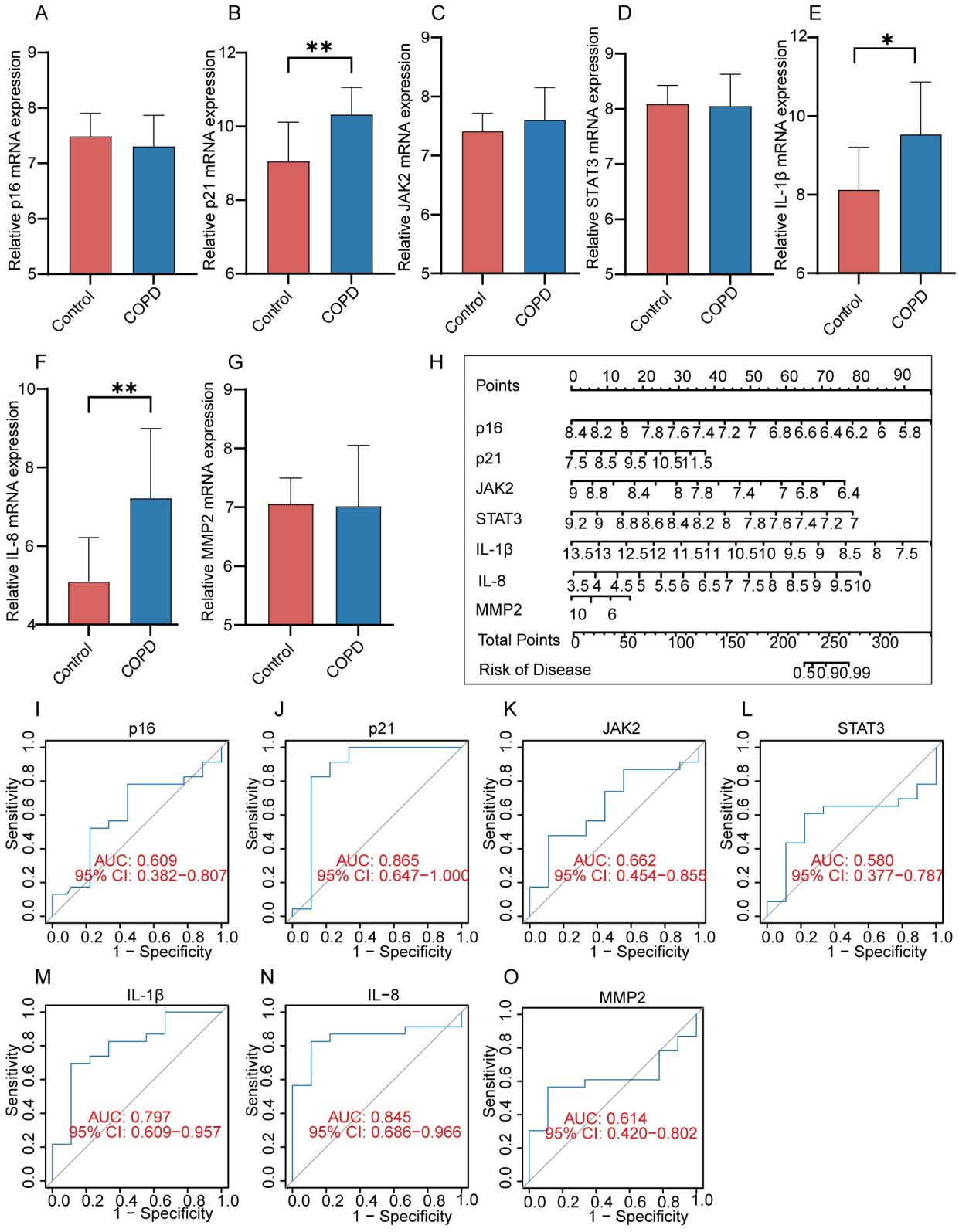


**Fig. 1. Differential analysis of 7 essential genes, nomogram, and evaluation of diagnostic value.** (A–G) mRNA expression levels of cyclin dependent kinase inhibitor 2a (*p16*), cyclin dependent kinase inhibitor 1a (*p21*), Janus kinase 2 (*JAK2*), signal transducer and activator of transcription 3 (*STAT3*), interleukin-1$\beta$ (*IL*-1$\beta$), interleukin-8 (*IL*-8), and matrix metalloproteinase 2 (*MMP2*). n > 3. (H) The nomogram of p16, p21, JAK2, STAT3, IL-1$\beta$, IL-8, and MMP2. (I–O) The area under the curve of p16, p21, JAK2, STAT3, IL-1$\beta$, IL-8, and MMP2. $^{*}p < 0.05$, $^{**}p < 0.01$ vs. Control. COPD, Chronic obstructive pulmonary disease.

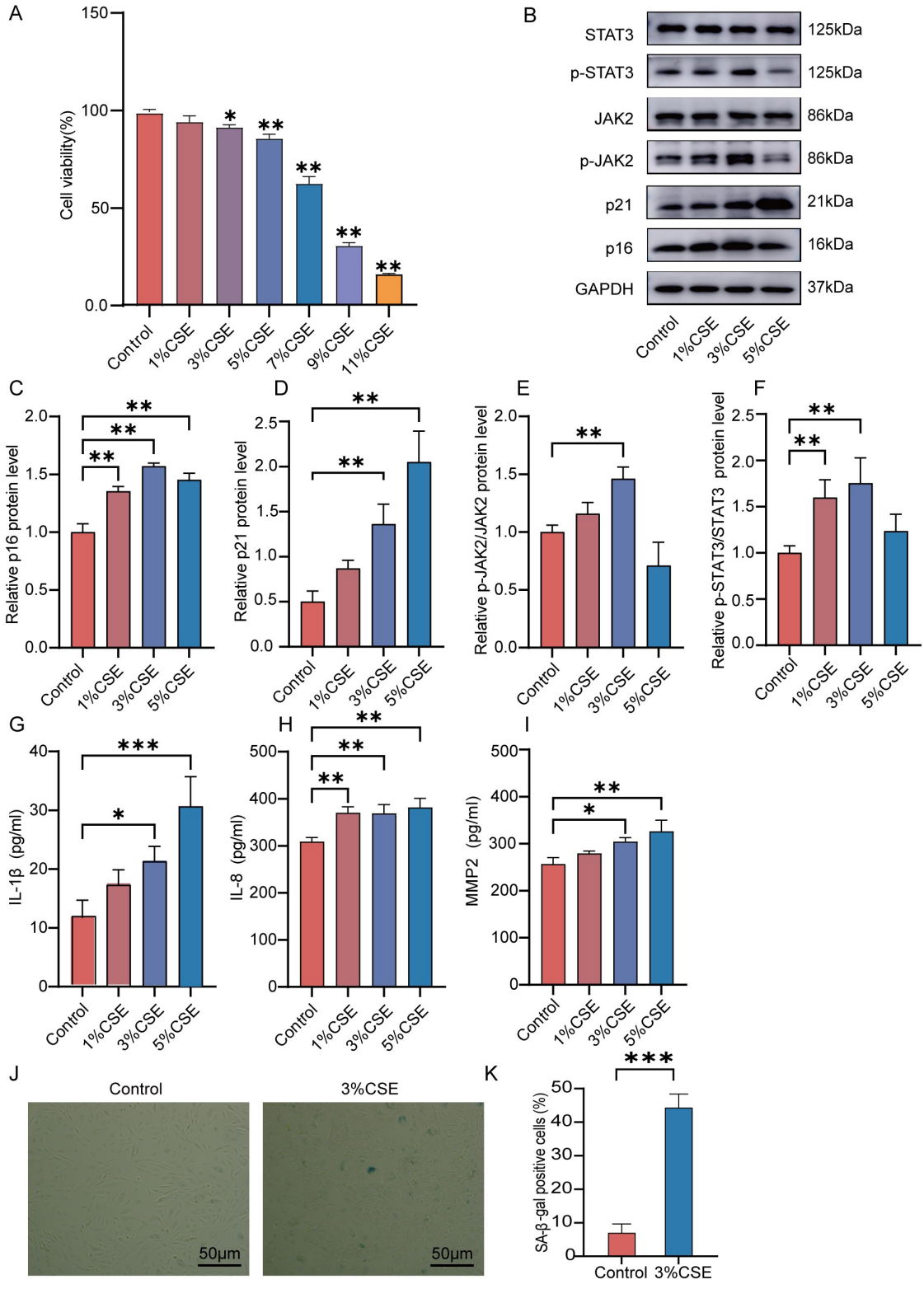


**Fig. 2. CSE treatment reduced the viability of BEAS-2B cells in a dose-dependent manner and activated the JAK2/STAT3 signaling pathway.** (A) The viability of BEAS-2B cells was assessed employing the Cell Counting Kit-8 (CCK-8) assay after 24 hours of CSE treatments. n = 3. (B–F) Protein expression levels of p16, p21, JAK2, phosphorylated-JAK2 (p-JAK2), STAT3, and phosphorylated-STAT3 (p-STAT3) were assessed using Western blot analysis following CSE treatment. GAPDH served as the internal control (n = 3). (G–I) IL-1$\beta$, IL-8, and MMP2 levels were examined in the supernatants of cell cultures using enzyme-linked immunosorbent assay (ELISA) (n = 3). (J) Images of stimulated BEAS-2B cells after $\beta$-galactosidase staining. n = 3. (K) The percentages of SA-$\beta$-gal positive cells. n = 3. $^{*}p < 0.05$, $^{**}p < 0.01$, $^{***}p < 0.001$ vs. Control. CSE, cigarette smoke extract.

Journal of
BIOLOGICAL REGULATORS
and Homeostatic Agents

## Results

### *Bioinformatic Identification of JAK2/STAT3 Signaling Pathway and Diagnostic Value of SASP in COPD*

Using bioinformatics approaches, we investigated p16, p21, and the JAK2/STAT3 pathway along with SASP factors (IL-1$\beta$, IL-8, MMP2), which are indicative of cellular senescence. Differential expression analysis of these genes in the GSE38794 COPD dataset revealed substantial differences in *p21* ($p < 0.01$), *IL-1*$\beta$ ($p < 0.05$), and *IL-8* ($p < 0.01$) between the COPD and control groups (Fig. 1B,E,F). *JAK2* and *STAT3* were found to be expressed at the gene level (Fig. 1C,D), so it was reasonable that there was no difference. *p16* and *MMP2* showed no significant difference between the 2 groups (Fig. 1A,G). Subsequently, we constructed the nomogram incorporating these seven essential genes (Fig. 1H). Furthermore, assessing their diagnostic significance, we created ROC curves to determine the AUC and 95% CI for each gene. As depicted in Fig. 1I–O, the outcomes were as follows: p16 (AUC: 0.609, 95% CI: 0.382–0.807), p21 (AUC: 0.865, 95% CI: 0.647–1.000), JAK2 (AUC: 0.662, 95% CI: 0.454–0.855), STAT3 (AUC: 0.580, 95% CI: 0.377–0.787), IL-1$\beta$ (AUC: 0.797, 95% CI: 0.609–0.957), IL-8 (AUC: 0.845, 95% CI: 0.686–0.966) and MMP2 (AUC: 0.614, 95% CI: 0.420–0.802). Notably, p21, IL-1$\beta$, and IL-8 exhibited higher diagnostic values.

### *CSE Induces Senescence of BEAS-2B*

We evaluated the impact of CSE exposure on the viability of BEAS-2B cells. For this purpose, CSE was applied in varying concentrations (0, 1%, 3%, 5%, 7%, and 11%) for 24 hours to determine the appropriate concentration of intervention. Following cellular treatment, their viability was assessed using CCK-8 assay (Fig. 2A). We observed that CSE concentrations lower than 5% did not influence the viability of BEAS-2B cells, however, it was significantly decreased at concentrations of 7%, 9%, and 11% ($p < 0.01$). Therefore, CSE at 1%, 3%, and 5% concentrations was selected for treating cells in the following experiments. To determine the impact of CSE on the senescence state of activated BEAS-2B cells, Western blot was used to assess the expression levels of senescence-associated chemicals. As shown in Fig. 2B–F, CSE treatment significantly increased the expression levels of p16 and p21 compared to the control. Specifically, treatment with 1%, 3%, and 5% CSE resulted in a significant increase in p16 expression ($p < 0.01$), with the highest elevation observed at 5% CSE. Moreover, CSE increased p21 expression in a concentration-dependent manner ($p < 0.01$), with the most prominent elevation at 5% CSE. Furthermore, we evaluated the impact of different concentrations of CSE on the JAK2/STAT3 signaling pathway. We observed that CSE at 3% significantly inhibited the levels of phosphorylated-JAK2 (p-JAK2) ($p < 0.01$) and phosphorylated-STAT3 (p-STAT3) ($p < 0.01$). However, CSE at 3% did not affect the total expression levels of JAK2 and STAT3. As p-JAK2 activation was found only at 3% CSE stimulation, we used this concentration as the intervention stimulus for subsequent experiments. Additionally, the levels of IL-1$\beta$ ($p < 0.05$), IL-8 ($p < 0.05$), and MMP2 ($p < 0.05$) were assessed utilizing ELISA, demonstrating significantly elevated cytokine levels after CSE exposure compared to the control group (Fig. 2G–I). Furthermore, after 24 hours of 3% CSE stimulation, the cells enlarged, and SA-$\beta$-gal activity increased, leading to a higher proportion of SA-$\beta$-gal positive cells ($p < 0.001$, Fig. 2J,K). These findings further confirm CSE-induced senescence in BEAS-2B cells.

### *JAK2/STAT3 Signaling Pathway Regulates CSE-Induced Senescence in BEAS-2B Cells*

To further assess the role of JAK2/STAT3 signaling in CSE-mediated activation of cellular senescence, we incubated the cells with or without the JAK2/STAT3 pathway inhibitor AG490 (10 μM) for 2 hours before 3% CSE treatment. Compared to the control group, CSE significantly elevated the expression of p16 ($p < 0.01$) and p21 ($p < 0.01$) and activated the JAK2/STAT3 signaling pathway ($p < 0.01$). However, treatment with AG490 significantly decreased p16 ($p < 0.05$) and p21 ($p < 0.05$) protein levels, as well as p-JAK2 ($p < 0.01$) and p-STAT3 ($p < 0.05$) compared to 3% CSE stimulation (Fig. 3A–E). Moreover, qRT-PCR revealed a significant reduction in p16 ($p < 0.01$) and p21 ($p < 0.01$) levels within AG490-treated BEAS-2B cells (Fig. 3F,G). Furthermore, as shown in Fig. 3H–J, AG490 pretreatment substantially reduced the concentrations of the SASP factors, including IL-1$\beta$ ($p < 0.05$), IL-8 ($p < 0.05$), and MMP2 ($p < 0.01$). Additionally, SA-$\beta$-gal activity and the proportion of positive cells were reduced ($p < 0.01$) compared to the 3% CSE (Fig. 3K,L). Overall, these findings suggest that CSE inhibits bronchial epithelial cell senescence by regulating the JAK2/STAT3 signaling pathway.

### *Sal Reduces CSE-Stimulated Cellular Senescence and Inhibits JAK2/STAT3 Signaling Pathway within BEAS-2B Cells*

To evaluate the impact of Sal on BEAS-2B cell viability, we treated the cells with varying concentrations of Sal (0, 5 μM, 10 μM, 20 μM, 40 μM, 80 μM, 160 μM, and 320 μM) for 24 hours. CCK-8 assay showed that the viability of BEAS-2B cells reduced below 80% when treated with a Sal concentration of up to 320 μM (Fig. 4A). Therefore, we selected Sal concentrations of 40 μM, 80 μM, and 160 μM for an 8-hour pretreatment of BEAS-2B cells. Sal treatment reduced the protein expression of markers linked to CSE-induced senescence, including p16 and p21 Fig. 4B–D. Both 80 μM and 160 μM showed significant differences ($p < 0.01$), while 40 μM did not exhibit substantial differences ($p > 0.05$). Furthermore, p-JAK2 and p-STAT3

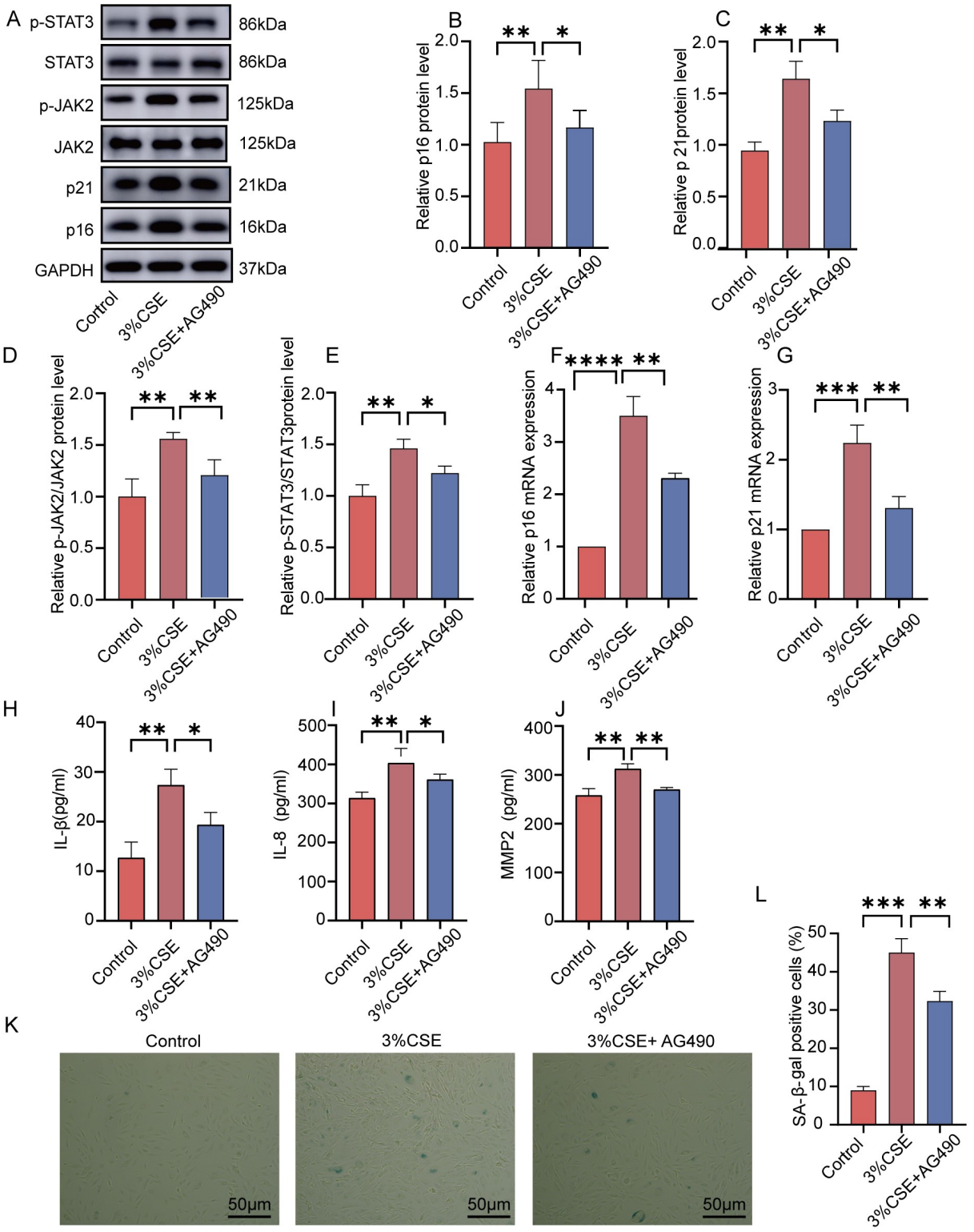


**Fig. 3. The JAK2/STAT3 signaling pathway contributes to CSE-induced senescence in BEAS-2B cells.** (A–E) The protein expression levels of p16, p21, JAK2, and STAT3 were determined using Western blot analysis. GAPDH served as the internal control. n = 3. (F,G) The mRNA expression levels of *p16* and *p21* in BEAS-2Bs were assessed using qRT-PCR. GAPDH served as the internal control. n = 3. (H–J) IL-1$\beta$, IL-8, and MMP2 levels were determined in the supernatants of cell cultures using Western blot analysis. n = 3. (K) Images of BEAS-2B cells after $\beta$-galactosidase staining following CSE and AG490 treatment. n = 3. (L) The percentages of SA-$\beta$-gal positive cells. n = 3. $^{*}p < 0.05$, $^{**}p < 0.01$, $^{***}p < 0.001$, $^{****}p < 0.0001$ vs. Control or 3% CSE. CSE, cigarette smoke extract.

Journal of
BIOLOGICAL REGULATORS
and Homeostatic Agents

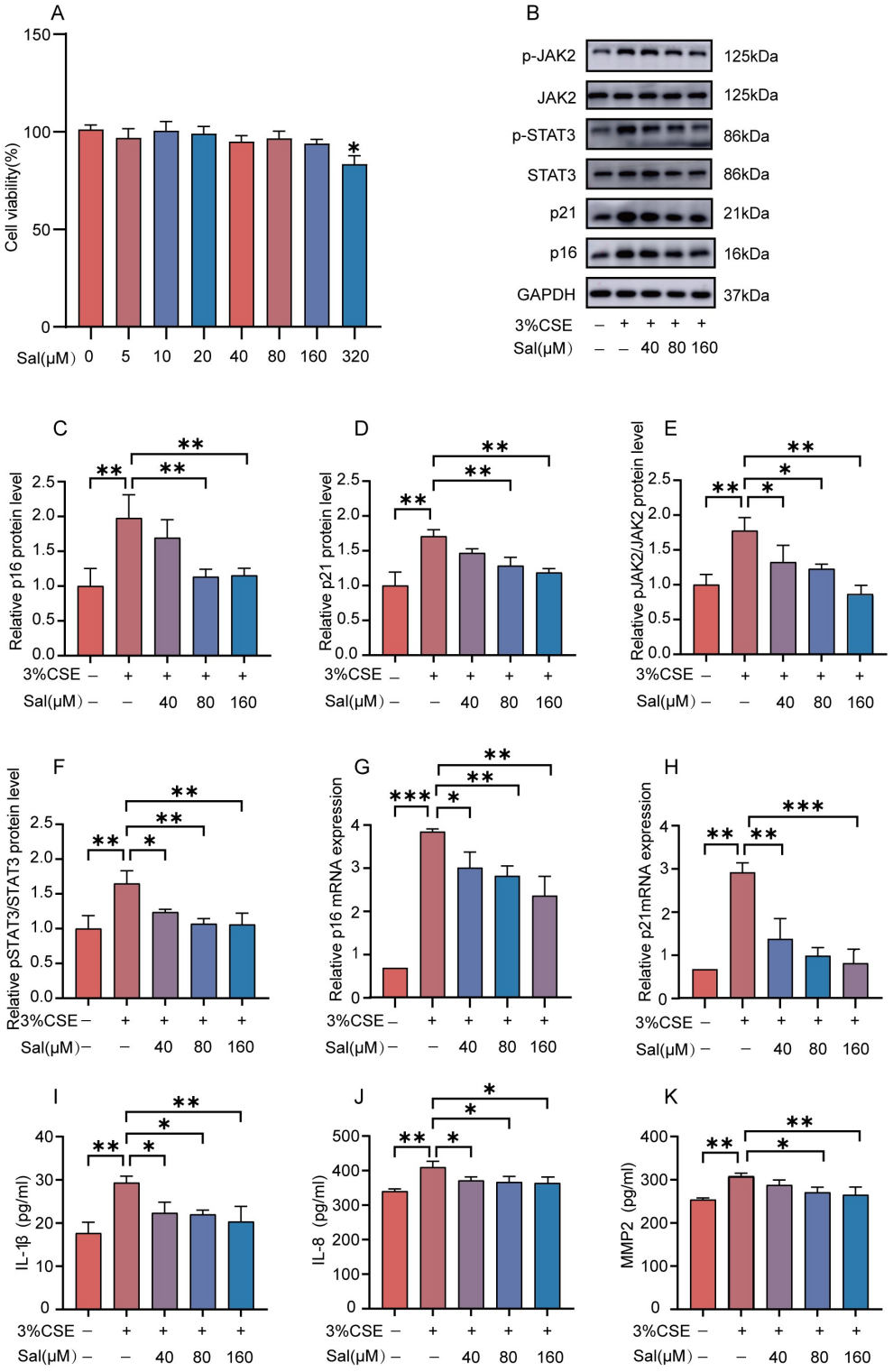


**Fig. 4. Sal inhibits CSE-mediated senescence of BEAS-2B cells by targeting the JAK2/STAT3 signaling pathway.** (A) The viability of BEAS-2B cell was assessed employing the CCK-8 assay after 24 hours of Sal treatments. n = 3. (B–F) The expression levels of p16, p21, JAK2, and STAT3 were determined using Western blot analysis. GAPDH served as the internal control. n = 3. (G,H) The mRNA expression levels of *p16* and *p21* in BEAS-2B were assessed using qRT-PCR after corresponding treatments. n = 3. (I–K) The levels of IL-1$\beta$, IL-8, and MMP2 proteins were evaluated using ELISA. n = 3. $^{*}p < 0.05$, $^{**}p < 0.01$, $^{***}p < 0.001$ vs. Control or 3% CSE. Sal, salidroside.

protein levels were reduced in a dose-dependent manner (Fig. 4B,E,F), with 40 μM, 80 μM, and 160 μM concentrations exhibiting significant differences compared to the CSE group ($p < 0.05$).

The findings from qRT-PCR indicated that *p16* and *p21* mRNA levels were substantially elevated in the Sal group compared to the CSE group ($p < 0.05$), with a more pronounced decrease in p21 (Fig. 4B,G,H). Concurrently, pretreatment with Sal resulted in a dose-dependent alleviation in the levels of IL-1$\beta$ ($p < 0.01$), IL-8 ($p < 0.05$), and MMP2 ($p < 0.05$) in CSE-treated cells (Fig. 4I–K). Furthermore, the proportion of SA-$\beta$-gal positive cells triggered by CSE was reduced in a dose-dependent manner by all pretreatments ($p < 0.01$) (**Supplementary Fig. 1A,B**). These findings imply that Sal protects BEAS-2B cells from cellular senescence induced by CSE. These findings further indicate that Sal may alleviate CSE-induced senescence in BEAS-2B cells by inhibiting the JAK2/STAT3 pathway.

## Discussion

Due to the advancement of high-throughput technologies and the rapid development of bioinformatics, there has been a considerable accumulation and expansion of biomedical data. Bioinformatics helps us comprehensively understand the essence of diseases from these massive clinical and experimental datasets [28]. Therefore, combining bioinformatics with experimental studies holds a prom to identify potential targets and reveal therapeutic mechanisms. In this study, bioinformatics analysis revealed the role of the JAK2/STAT3 signaling pathway in regulating COPD-associated cellular senescence.

The JAK2/STAT3 signaling pathway has been implicated in the development of senescence. JAK2/STAT3 signaling pathway induces cellular senescence by mediating SASP [15,29–31] and increasing the expression of senescence-associated markers, including p53, p21, p16, and SA-$\beta$-gal [32]. It has been found that activation of the interferon gene stimulating factor (STING) results in the phosphorylation of nuclear factor $\kappa$B (NF-$\kappa$B) through TANK-binding kinase 1 (TBK1) [33]. Furthermore, it has been shown that the NF-$\kappa$B signaling pathway is the predominant mechanism for generating the secretory phenotype linked with senescence (SASP) [34]. A specific inhibitor targeting the JAK2/STAT3 signaling pathway reduces cellular senescence and oxidative DNA damage in the brains of mice after ischaemic stroke by blocking cGAS/STING/NF-$\kappa$Bp65 [35]. Overexpression of the suppressor of cytokine signaling 5 (SOCS5) inhibits JAK2/STAT3 signaling-mediated oxidative stress in a mouse model of COPD [36]. Meanwhile, Sal-B promotes lung cell proliferation and migration through JAK2/STAT3 pathway [37]. It has been indicated that CSE induces M2 polarization in mouse macrophages through JAK2/STAT3 [38]. Beaulieu *et al*. [31] found that the JAK2 inhibitor rucotinib inhibited emphysema and reduced the expression of p16 and p21, as well as senescence of pulmonary artery smooth muscle cells in (PLA2R1-TG) transgenic mice. These results are consistent with our study. In the present study, AG490, an inhibitor targeting the JAK2/STAT3 pathway, significantly reduced p16 and p21 expression, $\beta$-galactosidase activity, and SASP (IL-1$\beta$, IL-8, MMP2) levels in senescent bronchial epithelial cells. These results suggest that the JAK2/STAT3 signaling pathway can induce senescence in bronchial epithelial cells through SASP production.

Sal, possessing a wide range of pharmacological properties, holds promise for the prevention and treatment of a variety of diseases. Hence, its immense clinical application in regulating the JAK2/STAT3 has been widely studied in tumors. Sal inhibits the level of phosphorylation of the JAK2/STAT3 signaling pathway in tumor cells, thereby inhibiting the proliferation of tumor cells [39–42]. Additionally, it inhibits angiogenesis by hindering the DNA-binding activity of STAT3 and preventing STAT3 binding to the new binding site of the *MMP2* gene promoter [43]. In inflammatory diseases, Sal has been shown to have an inhibitory impact on angiogenesis. During inflammatory responses, sal have been found to attenuate LPS-induced inflammation in an ex vivo lung injury model by inhibiting the phosphorylation of JAK2/STAT3 and subsequent nuclear translocation of STAT3 [44]. Liu *et al*. [45] reported that Sal affects Th17 cell differentiation by inhibiting the nuclear translocation of STAT3. Additionally, it was shown that Sal inhibition of JAK2/STAT3 signaling pathway attenuated the release of hypoxia-induced proinflammatory cytokine from the hepatic liver [46]. Previous studies suggest that Sal has the potential as a protective agent in a variety of lung diseases, including acute lung injury [47], pulmonary ischemia-reperfusion [48], and allergic asthma [49], primarily exerting its effects through anti-inflammatory mechanisms. However, no studies have revealed Sal's regulation of senescence through the JAK2/STAT3 signaling pathway. The results of *in vitro* experiments were consistent with the expected findings: Sal significantly inhibited the JAK2/STAT3 signaling pathway level in senescent bronchial epithelial cells, showing potential anti-aging properties.

The current study shows that Sal exhibits a favorable safety profile and oral bioavailability. The oral bioavailability of Sal in rats was 51.97%, although different conditions may affect the bioavailability of Sal [50]. However, various conditions may affect the bioavailability of rhodiola rosea. For example, in diabetic rats, the absorption of Sal was favored by diabetes [51]. In diabetic rats, for example, the absorption of rhodiola rosea was found to be selected. In contrast, in rats with myocardial ischemia, the absorption of Sal was reduced.

Pharmacokinetics showed that multiple administrations could increase the bioavailability of rhodiola rosea

Journal of
BIOLOGICAL REGULATORS
and Homeostatic Agents

[52]. Furthermore, Pharmacokinetics findings show that the efficacy of Sal can be improved through various methods. Moreover, the absorption of rhodiola rosea can be affected by different drugs [53]. Similarly, the absorption of Sal can be affected by multiple medications. Moreover, there are limited studies on the toxicity of Sal, but studies on rhodiola rosea herbs have shown that Sal displays a high level of safety in animal models, even with both short-term and long-term administration [54,55]. Additionally, a study on rhodiola rosea soft capsules has demonstrated that these capsules are safe and non-toxic [56]. Study on Sal using the model of adriamycin-induced cardiotoxicity by Zhang *et al*. [57] showed that Sal did not induce clinical adverse events throughout the treatment period. Additionally, research has indicated that rhodioloside does not show genotoxicity in mice [58]. Similarly, we observed that Sal was not genotoxic in mice. These studies reveal that Sal exhibits low toxicity and high oral utilization.

It is crucial to acknowledge the limitations of this study. Firstly, *in vitro* utilization of JAK2 siRNA and *in vivo* knockdown of JAK2 in lung tissues could aid in investigating the role of JAK2/STAT3 signaling in promoting CSE-mediated cellular senescence by Sal. Additionally, the *in vivo* safety profile of Sal has not been explored. There is a need to explore strategies to increase the bioavailability of Sal in future investigations. Secondly, our study only explored the protective impact of Sal through the activation of the JAK2/STAT3 signaling. The therapeutic efficacy of Sal may involve a series of complex signaling pathways.

## Conclusion

In conclusion, our study provides evidence that Sal attenuates CSE-induced senescence in BEAS-2B cells by inhibiting the JAK2/STAT3 signaling pathway. These findings offer critical new insights into understanding the protective role of Sal against cellular senescence and its underlying mechanisms.

## Availability of Data and Materials

The dataset analyzed for this study can be found at the https://www.ncbi.nlm.nih.gov/geo/query/acc.cgi?acc=GSE38974.

## Author Contributions

LL, WL designed the research study. LL and WF performed the research. LL and JW provided help and advice on the experiments. SZ analyzed the data. All authors contributed to editorial changes in the manuscript. All authors read and approved the final manuscript. All authors have participated sufficiently in the work and agreed to be accountable for all aspects of the work.

## Ethics Approval and Consent to Participate

Not applicable.

## Acknowledgment

Not applicable.

## Funding

This research received no external funding.

## Conflict of Interest

The authors declare no conflict of interest.

## Supplementary Material

Supplementary material associated with this article can be found, in the online version, at https://doi.org/10.23812/j.biol.regul.homeost.agents.20243805.351.

## References

[1] López-Campos JL, Tan W, Soriano JB. Global burden of COPD. Respirology. 2016; 21: 14–23.
[2] Agustí A, Celli BR, Criner GJ, Halpin D, Anzueto A, Barnes P, *et al*. Global Initiative for Chronic Obstructive Lung Disease 2023 Report: GOLD Executive Summary. Archivos De Bronconeumologia. 2023; 59: 232–248.
[3] Barnes PJ, Baker J, Donnelly LE. Cellular Senescence as a Mechanism and Target in Chronic Lung Diseases. American Journal of Respiratory and Critical Care Medicine. 2019; 200: 556–564.
[4] Jarhyan P, Hutchinson A, Khaw D, Prabhakaran D, Mohan S. Prevalence of chronic obstructive pulmonary disease and chronic bronchitis in eight countries: a systematic review and meta-analysis. Bulletin of the World Health Organization. 2022; 100: 216–230.
[5] Aoshiba K, Zhou F, Tsuji T, Nagai A. DNA damage as a molecular link in the pathogenesis of COPD in smokers. The European Respiratory Journal. 2012; 39: 1368–1376.
[6] Huang W, Hickson LJ, Eirin A, Kirkland JL, Lerman LO. Cellular senescence: the good, the bad and the unknown. Nature Reviews. Nephrology. 2022; 18: 611–627.
[7] Birch J, Gil J. Senescence and the SASP: many therapeutic avenues. Genes & Development. 2020; 34: 1565–1576.
[8] Postma DS, Rabe KF. The Asthma-COPD Overlap Syndrome. The New England Journal of Medicine. 2015; 373: 1241–1249.
[9] Casanova JL, Holland SM, Notarangelo LD. Inborn errors of human JAKs and STATs. Immunity. 2012; 36: 515–528.
[10] Villarino AV, Kanno Y, O'Shea JJ. Mechanisms and consequences of Jak-STAT signaling in the immune system. Nature Immunology. 2017; 18: 374–384.
[11] Chen B, Ning K, Sun ML, Zhang XA. Regulation and therapy, the role of JAK2/STAT3 signaling pathway in OA: a systematic review. Cell Communication and Signaling. 2023; 21: 67.
[12] Kuilman T, Michaloglou C, Vredeveld LCW, Douma S, van Doorn R, Desmet CJ, *et al*. Oncogene-induced senescence relayed by an interleukin-dependent inflammatory network. Cell. 2008; 133: 1019–1031.
[13] Acosta JC, O'Loghlen A, Banito A, Guijarro MV, Augert A,

Raguz S, *et al*. Chemokine signaling via the CXCR2 receptor reinforces senescence. Cell. 2008; 133: 1006–1018.

[14] Barnes PJ. Senescence in COPD and Its Comorbidities. Annual Review of Physiology. 2017; 79: 517–539.

[15] Wu W, Fu J, Gu Y, Wei Y, Ma P, Wu J. JAK2/STAT3 regulates estrogen-related senescence of bone marrow stem cells. The Journal of Endocrinology. 2020; 245: 141–153.

[16] Zhou H, Huang B, Du J, Wang L. Role of the JAK2/STAT pathway and losartan in human glomerular mesangial cell senescence. Molecular Medicine Reports. 2010; 3: 393–398.

[17] Farr JN, Xu M, Weivoda MM, Monroe DG, Fraser DG, Onken JL, *et al*. Targeting cellular senescence prevents age-related bone loss in mice. Nature Medicine. 2017; 23: 1072–1079.

[18] Xiong J, Wang C, Chen H, Hu Y, Tian L, Pan J, *et al*. A$\beta$-induced microglial cell activation is inhibited by baicalin through the JAK2/STAT3 signaling pathway. The International Journal of Neuroscience. 2014; 124: 609–620.

[19] Chen J, Xu T, Zhu D, Wang J, Huang C, Lyu L, *et al*. Egg antigen p40 of Schistosoma japonicum promotes senescence in activated hepatic stellate cells by activation of the STAT3/p53/p21 pathway. Cell Death & Disease. 2016; 7: e2315.

[20] Zhuang W, Yue L, Dang X, Chen F, Gong Y, Lin X, *et al*. Rosenroot (*Rhodiola*): Potential Applications in Aging-related Diseases. Aging and Disease. 2019; 10: 134–146.

[21] Zhang J, Zhen YF, Pu-Bu-Ci-Ren, Song LG, Kong WN, Shao TM, *et al*. Salidroside attenuates beta amyloid-induced cognitive deficits via modulating oxidative stress and inflammatory mediators in rat hippocampus. Behavioural Brain Research. 2013; 244: 70–81.

[22] Zhang X, Zhang Y, Li R, Zhu L, Fu B, Yan T. Salidroside ameliorates Parkinson's disease by inhibiting NLRP3-dependent pyroptosis. Aging. 2020; 12: 9405–9426.

[23] Sun L, Dou F, Chen J, Chi H, Xing S, Liu T, *et al*. Salidroside slows the progression of EA.hy926 cell senescence by regulating the cell cycle in an atherosclerosis model. Molecular Medicine Reports. 2018; 17: 257–263.

[24] Xing SS, Li J, Chen L, Yang YF, He PL, Li J, *et al*. Salidroside attenuates endothelial cellular senescence via decreasing the expression of inflammatory cytokines and increasing the expression of SIRT3. Mechanisms of Ageing and Development. 2018; 175: 1–6.

[25] Mao GX, Xing WM, Wen XL, Jia BB, Yang ZX, Wang YZ, *et al*. Salidroside protects against premature senescence induced by ultraviolet B irradiation in human dermal fibroblasts. International Journal of Cosmetic Science. 2015; 37: 321–328.

[26] Du Y, Ding Y, Shi T, He W, Mei Z, Feng X, *et al*. Suppression of circXPO1 attenuates cigarette smoke-induced inflammation and cellular senescence of alveolar epithelial cells in chronic obstructive pulmonary disease. International Immunopharmacology. 2022; 111: 109086.

[27] Gou M, Qian N, Zhang Y, Wei L, Fan Q, Wang Z, *et al*. Construction of a nomogram to predict the survival of metastatic gastric cancer patients that received immunotherapy. Frontiers in Immunology. 2022; 13: 950868.

[28] Li X, Wei S, Niu S, Ma X, Li H, Jing M, *et al*. Network pharmacology prediction and molecular docking-based strategy to explore the potential mechanism of Huanglian Jiedu Decoction against sepsis. Computers in Biology and Medicine. 2022; 144: 105389.

[29] Ji T, Chen M, Sun W, Zhang X, Cai H, Wang Y, *et al*. JAK-STAT signaling mediates the senescence of cartilage-derived stem/progenitor cells. Journal of Molecular Histology. 2022; 53: 635–643.

[30] Chen M, Xiao L, Dai G, Lu P, Zhang Y, Li Y, *et al*. Inhibition of JAK-STAT Signaling Pathway Alleviates Age-Related Phenotypes in Tendon Stem/Progenitor Cells. Frontiers in Cell and Developmental Biology. 2021; 9: 650250.

[31] Beaulieu D, Attwe A, Breau M, Lipskaia L, Marcos E, Born E, *et al*. Phospholipase A2 receptor 1 promotes lung cell senescence and emphysema in obstructive lung disease. The European Respiratory Journal. 2021; 58: 2000752.

[32] Fang X, Huang W, Sun Q, Zhao Y, Sun R, Liu F, *et al*. Melatonin attenuates cellular senescence and apoptosis in diabetic nephropathy by regulating STAT3 phosphorylation. Life Sciences. 2023; 332: 122108.

[33] Abe T, Barber GN. Cytosolic-DNA-mediated, STING-dependent proinflammatory gene induction necessitates canonical NF-$\kappa$B activation through TBK1. Journal of Virology. 2014; 88: 5328–5341.

[34] Lopes-Paciencia S, Saint-Germain E, Rowell MC, Ruiz AF, Kalegari P, Ferbeyre G. The senescence-associated secretory phenotype and its regulation. Cytokine. 2019; 117: 15–22.

[35] Zhang W, Xu M, Chen F, Su Y, Yu M, Xing L, *et al*. Targeting the JAK2-STAT3 pathway to inhibit cGAS-STING activation improves neuronal senescence after ischemic stroke. Experimental Neurology. 2023; 368: 114474.

[36] Lei Y, He J, Hu F, Zhu H, Gu J, Tang L, *et al*. Sequential inspiratory muscle exercise-noninvasive positive pressure ventilation alleviates oxidative stress in COPD by mediating SOCS5/JAK2/STAT3 pathway. BMC Pulmonary Medicine. 2023; 23: 385.

[37] Dhapare S, Sakagami M. Salvianolic acid B as an anti-emphysema agent I: In vitro stimulation of lung cell proliferation and migration, and protection against lung cell death, and in vivo lung STAT3 activation and VEGF elevation. Pulmonary Pharmacology & Therapeutics. 2018; 53: 107–115.

[38] Yuan F, Fu X, Shi H, Chen G, Dong P, Zhang W. Induction of murine macrophage M2 polarization by cigarette smoke extract via the JAK2/STAT3 pathway. PLoS ONE. 2014; 9: e107063.

[39] Sun KX, Xia HW, Xia RL. Anticancer effect of salidroside on colon cancer through inhibiting JAK2/STAT3 signaling pathway. International Journal of Clinical and Experimental Pathology. 2015; 8: 615–621.

[40] Lv C, Huang Y, Liu ZX, Yu D, Bai ZM. Salidroside reduces renal cell carcinoma proliferation by inhibiting JAK2/STAT3 signaling. Cancer Biomarkers: Section a of Disease Markers. 2016; 17: 41–47.

[41] Huang L, Huang Z, Lin W, Wang L, Zhu X, Chen X, *et al*. Salidroside suppresses the growth and invasion of human osteosarcoma cell lines MG63 and U2OS in vitro by inhibiting the JAK2/STAT3 signaling pathway. International Journal of Oncology. 2019; 54: 1969–1980.

[42] Shang H, Wang S, Yao J, Guo C, Dong J, Liao L. Salidroside inhibits migration and invasion of poorly differentiated thyroid cancer cells. Thoracic Cancer. 2019; 10: 1469–1478.

[43] Kang DY, Sp N, Kim DH, Joung YH, Lee HG, Park YM, *et al*. Salidroside inhibits migration, invasion and angiogenesis of MDA MB 231 TNBC cells by regulating EGFR/Jak2/STAT3 signaling via MMP2. International Journal of Oncology. 2018; 53: 877–885.

[44] Qi Z, Qi S, Ling L, Lv J, Feng Z. Salidroside attenuates inflammatory response via suppressing JAK2-STAT3 pathway activation and preventing STAT3 transfer into nucleus. International Immunopharmacology. 2016; 35: 265–271.

[45] Liu Z, Chen L, Xiong D, Zhan Y, Liu J, Ouyang L, *et al*. Salidroside affects the Th17/Treg cell balance in aplastic anemia via the STAT3/HIF-1$\alpha$/ROR$\gamma$t pathway. Redox Report: Communications in Free Radical Research. 2023; 28: 2225868.

[46] Xiong Y, Wang Y, Xiong Y, Teng L. Protective effect of Salidroside on hypoxia-related liver oxidative stress and inflammation via Nrf2 and JAK2/STAT3 signaling pathways. Food Science & Nutrition. 2021; 9: 5060–5069.

Journal of
BIOLOGICAL REGULATORS
and Homeostatic Agents

[47] Song D, Zhao M, Feng L, Wang P, Li Y, Li W. Salidroside attenuates acute lung injury via inhibition of inflammatory cytokine production. Biomedicine & Pharmacotherapy. 2021; 142: 111949.

[48] Wang Y, Chen Z, Luo J, Zhang J, Sang AM, Cheng ZS, *et al*. Salidroside postconditioning attenuates ferroptosis-mediated lung ischemia-reperfusion injury by activating the Nrf2/SLC7A11 signaling axis. International Immunopharmacology. 2023; 115: 109731.

[49] Cai H, Wang J, Mo Y, Ye L, Zhu G, Song X, *et al*. Salidroside suppresses group 2 innate lymphoid cell-mediated allergic airway inflammation by targeting IL-33/ST2 axis. International Immunopharmacology. 2020; 81: 106243.

[50] Guo N, Hu Z, Fan X, Zheng J, Zhang D, Xu T, *et al*. Simultaneous determination of salidroside and its aglycone metabolite p-tyrosol in rat plasma by liquid chromatography-tandem mass spectrometry. Molecules. 2012; 17: 4733–4754.

[51] He YX, Liu XD, Wang XT, Liu X, Wang GJ, Xie L. Sodium-dependent Glucose Transporter Was Involved in Salidroside Absorption in Intestine of Rats. Chinese Journal of Natural Medicines. 2009; 7: 444–448.

[52] Gu HL, Sun RB, Fei F, Li-Xiang A, Gao HX, Tao MX, *et al*. Salidroside shows a particular pharmacokinetic property in model rats of myocardial ischemia. Chinese Herbal Medicines. 2018; 10: 169–176.

[53] Li ZY, Li Q, Lü J, Ling JH, Yu XH, Chen XH, *et al*. LC-MS determination and pharmacokinetic study of salidroside in rat plasma after oral administration of suspensions of traditional Chinese medicine *Erzhi Wan* and Fructus *Ligustri lucidi*. Journal of Pharmaceutical Analysis. 2011; 1: 8–12.

[54] Lorke D. A new approach to practical acute toxicity testing. Archives of Toxicology. 1983; 54: 275–287.

[55] Larosa DF, Orange JS. 1. Lymphocytes. The Journal of Allergy and Clinical Immunology. 2008; 121: S364–S369; quiz S412.

[56] Darbinyan V, Aslanyan G, Amroyan E, Gabrielyan E, Malmström C, Panossian A. Clinical trial of Rhodiola rosea L. extract SHR-5 in the treatment of mild to moderate depression. Nordic Journal of Psychiatry. 2007; 61: 343–348.

[57] Zhang H, Shen WS, Gao CH, Deng LC, Shen D. Protective effects of salidroside on epirubicin-induced early left ventricular regional systolic dysfunction in patients with breast cancer. Drugs in R&D. 2012; 12: 101–106.

[58] Zhu J, Wan X, Zhu Y, Ma X, Zheng Y, Zhang T. Evaluation of salidroside in vitro and in vivo genotoxicity. Drug and Chemical Toxicology. 2010; 33: 220–226.